doi:10.1017/S1431927613003693
Microsc. Microanal. 19 (Suppl 2), 2013

Electronic Signature of Magnetic Moment and Fe-Vacancy Order in Fe-Based $TlFe_{1.6}Se_2$ Investigated by STEM/EELS

C. Cantoni, A. F. May, J. E. Mitchell, A. S. Sefat, M. A. McGuire, and B. C. Sales

Materials Science & Technology Division, Oak Ridge National Laboratory, Oak Ridge, TN 37831

The recently discovered $A_xFe_ySe_2$ superconductors with T_C in excess of 30K have attracted much interest given their differences from other Fe-based superconductors [1]. Although their crystal structure is very similar to that of 122 arsenides such as $BaFe_2As_2$ with the $ThCr_2Si_2$ structure, Fe vacancies are also present and often ordered according to a $\sqrt{5}a \times \sqrt{5}a$ supercell [2]. The Fe vacancies order below a temperature in the range of 460 -580 K. At the same temperature or slightly below, the spins align in a block-checkerboard antiferromagnetic structure (BCAF) with the direction of the spins along the *c*-axis and a local magnetic moment of ~ $3.3\mu_B$/Fe. $A_xFe_ySe_2$ are air sensitive and superconducting samples have not been to date synthesized as a pure, homogeneous phase. Phase separation is always observed at the micron or nanoscale with magnetic and superconducting phases finely intermixed [3]. The two phases show matching crystal structure and are coherently distributed, the one differing from the other only by the presence and/or order of Fe-vacancies. Although it has been proposed that the superconducting phase does not contain Fe vacancies [4], superconductivity is only observed in samples containing regions with vacancy and magnetic order. Here we investigate the nature of phase separation in $TlFe_{1.6}Se_2$ single crystals and its electronic signature by electron energy loss spectroscopy (EELS) in the aberration corrected scanning transmission electron microscope (STEM). By comparing the Fe-$L_{2,3}$ edge fine structure with other Fe-based compounds we derive qualitative trends for the local magnetic moment and the crystal fields of different Fe-based families.

Although $TlFe_{1.6}Se_2$ is not superconducting, its crystal and magnetic structures are similar to the superconducting compositions in which Tl is in part or entirely replaced by K, Cs, or Rb. On the other hand, $TlFe_{1.6}Se_2$ is less air sensitive and forms a "cleaner" system, in the sense that unlike for the alkali-metal-containing counterparts, the Tl site is always fully occupied and the Fe content shows little variation, reducing the possibility of spurious phases and allowing for better studying the magnetic insulating phase, which is thought to be the parent compound for the superconducting phase. Depending on the initial composition and processing conditions, $TlFe_{1.6}Se_2$ single crystals can be grown in two variants, one showing a nanoscale phase separation into regions with ordered and disordered Fe vacancies, respectively, and another variant showing complete and homogeneous order of Fe vacancies with the $\sqrt{5}a \times \sqrt{5}a$ superstructure. Figures 1a)-b) show HAADF images for the two variants obtained along the [130] and [210] of the $ThCr_2Si_2$ subcell. Previous magnetization and neutron scattering measurements have shown that these two (same composition) variants have different magnetic ground states [5]. In the fully ordered sample, after the spins align in the BCAF structure at 460 K a second transition occurs at 100 K, which flips the spins within the *ab* planes. On the other hand, in the phase-separated sample only a spin canting towards the *ab* planes at 140 K is observed and subsequently, as the temperature is reduced to ~100 K, the BCAF structure is recovered. We interpret such behavior for the phase separated sample as originating from the elastic interaction between ordered and disordered regions, which show significantly different lattice parameters along *c* and are therefore strain coupled, as shown in Fig. 1c) by the map of the ε_{yy} strain component calculated from an HAADF image using geometrical phase analysis (GPA).

We analyzed the Fe-$L_{2,3}$ EELS edge of both phase-separated and fully ordered $TlFe_{1.6}Se_2$ samples and compared those to the Fe-$L_{2,3}$ edges of different Fe-based compounds: the chalcogenide superconductor $Fe_{0.99}Te_{0.55}Se_{0.45}$, and the 122 parent $BaFe_2As_2$. Fig. 1 d) shows a plot of the $L_{2,3}$ ratio calculated using the Pearson method [6] for the four samples after the background in the raw spectra was removed, the spectra deconvolved using the Fourier-ratio method and the contribution from transitions to the continuum removed using a Hartree-Slater-type step function. In the same plot, the measured magnetic moments for the two $TlFe_{1.6}Se_2$ samples are reported on the right "*y*" axis together with local magnetic moments extracted from the literature for $FeTe_xSe_{2-x}$ and $BaFe_2As_2$ [7,8]. The data suggest a relationship of proportionality between the magnetic moment of the samples studied and their EELS $L_{2,3}$ ratio. This interesting finding can be explained by recalling that the $L_{2,3}$ ratio in transition metals is dependent on the ion's oxidation state, crystal field (or ion bonding environment), and spin state. In all the materials considered here, Fe is expected to be in the +2 oxidation state and in tetrahedral coordination with a similar anion environment. Although distortions from a perfect tetrahedral field are expected with different magnitude in different Fe-based compounds, these distortions should produce negligible changes in the integrated intensities of the L_2 and L_3 edges as compared to the changes produced by different spin states. As a consequence, the data in Fig. 1 d) suggest $A_xFe_ySe_2$, $FeTe_xSe_{2-x}$, and 122 arsenides have different spin states, providing an explanation for their different local magnetic moments as experimentally measured by X-ray and photo electron spectroscopy. Crystal field effects are displayed by additional structure or broadening of the L_3 edge caused by additional peaks close in energy to the edge threshold. Fig. 1 e) shows these effects for $TlFe_{1.6}Se_2$, $Fe_{0.99}Te_{0.55}Se_{0.45}$ and $BaFe_2As_2$ and indicates that $TlFe_{1.6}Se_2$ displays the largest crystal field of all three compounds, in agreement with theoretical calculation for $A_xFe_ySe_2$ materials [9, 10].

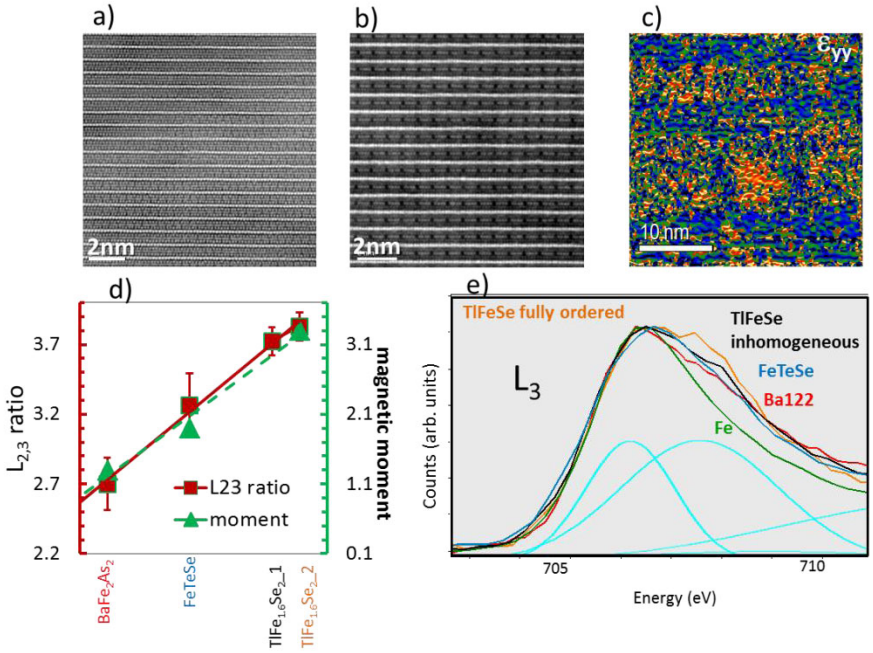

Fig. 1. a) and b), HAADF images of the phase-separated and fully ordered $TlFe_{1.6}Se_2$ crystals. c) strain yy component for the phase separated $TlFe_{1.6}Se_2$ crystal (blue: ordered phase; orange: disordered phase. d) plot of the L23 ratio and corresponding magnetic moment . e) plot of the L_3 edge for the different compounds studied (see text).

[1] E. Dagotto arXiv: 1210.6501 (2012)
[2] F. Ye *et al*. Phys. Rev. Lett. 107, 137003 (2011)
[3] F. Chen, *et al*. Phys. Rev. X 1, 021020 (2011)
[4] W. Li *et al.* Nat. Phys. 8, 126 (2012)
[5] A. F. May *et al*. Phys. Rev. Lett.
[6] D. H. Pearson Phys. Rev. B 47, 8471 (1993)
[7] H. Gretarsson *et al.* Phys. Rev. B 84, 100509(R) (2011)
[8] P. Vilmercati *et al*. Phys. Rev. B 85, 220503(R) (2012)
[9] Z. P. Yin, K. Haule, and G. Kotliar Nat. Mater. 10, 932 (2011).
[10] Research supported by the Materials Sciences and Engineering Division,Office of Science, US Department of Energy.

https://doi.org/10.1017/S1431927613003693 Published online by Cambridge University Press